Available online at www.sciencedirect.com
SCIENCE DIRECT
Catalysis Today 113 (2006) 251–256
CATALYSIS TODAY
www.elsevier.com/locate/cattod

# Electrical and optical study of Cu(In, Ga)$Se_2$ co-evaporated thin films

A. Amara [a,*], A. Ferdi [a], A. Drici [a], J.C. Bernède [b], M. Morsli [b], M. Guerioune [a]

[a] *LEREC, Département de Physique, Université de Annaba, BP12 Annaba, Algeria*
[b] *LPSE-FSTN, Université de Nantes, 2 rue de la Houssinière, PB 92208, 44322 Nantes Cedex 3, France*

Available online 19 January 2006

**Abstract**

Co-evaporation technique from three sources was used to prepare Cu(In, Ga)$Se_2$ polycrystalline thin films for photovoltaic conversion. Their conductivity was studied in the range 20–300 K. The grain boundary scattering mechanism is mainly responsible for the diffusion process in the latter materials. In the low temperature region, we interpret the data in terms of Mott law and the analysis is very consistent with the variable range hopping. However, thermoionic emission is predominant at high temperatures. When the conductivity deviates from the classical grain boundary conduction models, inhomogeneity is then considered and parameters such as the standard deviation and the mean potential barrier height are derived. Transmittance measurements yielded band gap values of 1.07 and 1.64 eV for $CuInSe_2$ and $CuGaSe_2$, respectively.


*Keywords:* Conductivity; Grain boundary; Cu(In, Ga)$Se_2$

## 1. Introduction

As environmental and energy resource concerns have increased in recent years, greater attention has been given to the I–III–$VI_2$-type ternary compounds, to develop renewable energy sources such as photovoltaic electric generators [1,2]. Ternary semiconductors of the type I–III–$VI_2$ have received considerable attention because of their potential applications in optoelectronic devices [1,2]. $CuInSe_2$ and $CuGaSe_2$ have a chalcopyrite structure and band gaps of 1.04 and 1.7 eV [3,4], respectively. The mixed compounds of the latter materials are leading candidates as absorbers in solar cells [5,6]. $CuIn_{1-x}Ga_xSe_2$ based solar cells have shown efficiencies as high as 19% [7] with no evidence of degradation of the absorber layer with time or light exposure. Thus the investigation of some fundamental properties of both compounds is necessary in determining the efficiency of the resulting solar cells.

In this study, we present electrical and optical measurements of co-evaporated Cu(In, Ga)$Se_2$ thin films. The electrical data have been interpreted in relation with the polycrystalline nature of these materials. The optical measurements have shown that the latter materials characteristics namely their direct band gaps and high absorption ($\alpha \sim 10^5\ cm^{-1}$) coefficients are very suitable for solar cells fabrication.

## 2. Experimental procedure

Polycrystalline Cu(In, Ga)$Se_2$ films; i.e. $CuIn_{1-x}Ga_xSe_2$ films, have been deposited by three sources evaporation of Cu, In–Ga and Se using simple tungsten boats. In a first time, elemental fluxes were independently, and successively, calibrated by measuring each deposition rate with a quartz monitor. Then the deposition rates were controlled by the source temperature. The whole deposition time was 25 min. The evaporation sources being simple tungsten boats, a precise control of the flux was quite difficult and, to avoid large deviation from the expected final composition, each element was weighted in order to be sure to approach the desired stoichiometry. During the deposition, the evaporation rates were around 0.1 n $ms^{-1}$ for the metals and 2–3 n $ms^{-1}$ for Se. The substrates were cleaned using soap and deionised water. Before they are introduced into a vacuum apparatus, they were dried with $N_2$ gas. A detailed description of the optimum

* Corresponding author.
*E-mail address:* a.ama@caramail.com (A. Amara).

0920-5861/$ – see front matter © 2005 Elsevier B.V. All rights reserved.
doi:10.1016/j.cattod.2005.11.074

conditions and the evaporation process are described in [8]. Particularly in the case of the mixed compound $CuIn_{1-x}Ga_xSe_2$, different combinations of the metal sources have been tested using three (Cu, In, Ga) and two (Cu + Ga, In or Cu, In + Ga or Cu + Ga, Cu + In) metal sources, while an independent source is systematically used for Se evaporation. In our latter study, electron probe microanalysis (EPMA), scanning electron microscopy (SEM) and X-ray photoelectron spectroscopy (XPS) analyses were performed on the films, and it was revealed that reproducible results can be achieved when the two alloy sources (Cu + Ga and In + Ga) are used. The different elements are homogeneously distributed all over the thickness of the films and the composition does not vary strongly in the bulk, with atomic percentages of the different elements in the same order of magnitude than the one measured by EPMA. Homogeneous films of thickness of 1 μm were deposited onto smooth bare or Mo coated soda lime glass (SLG) at a substrate temperature of 500 °C.

The films have been characterized by X-ray diffraction (XRD) by means of a Siemens D-500 diffractometer using the Cu $K\alpha_1$ radiation source ($\lambda = 0.15406$ nm) (PLC-IMN).

The dc conductivity was measured in the dark, using an electrometer (Kheithley 617). Ohmic contacts were prepared by evaporated gold dots.

The transmission of the materials was measured (by steps of 1 nm) at room temperature using a Cary 2300 spectrophotometer.

## 3. Results and discussion

### 3.1. X-ray diffraction

Figs. 1 and 2 show X-ray spectra of both $CuInSe_2$ and $CuGaSe_2$ thin films, respectively. No separate phase of other compounds was observed within the detection limits of XRD analysis. Both of the materials are polycrystalline in nature with a chalcopyrite structure. They exhibited preferential growth film crystallites corresponding to (1 1 2) planes.

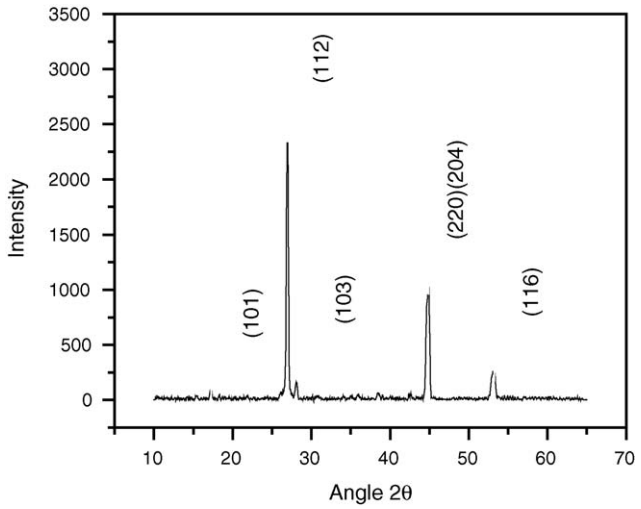


Fig. 1. $CuInSe_2$ X-ray diffraction spectra.

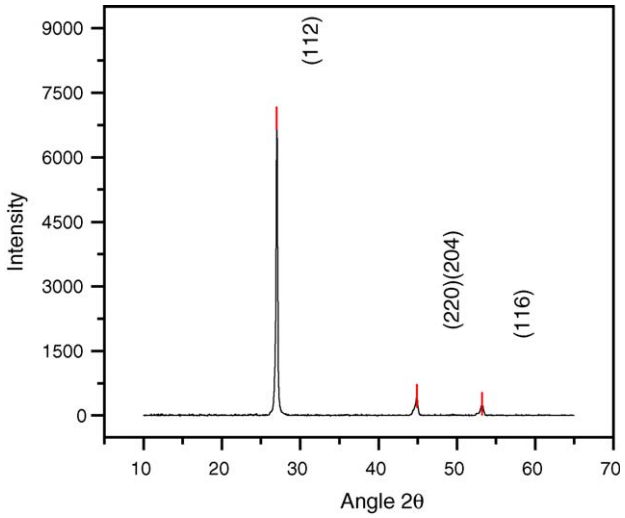


Fig. 2. $CuGaSe_2$ X-ray diffraction spectra.

The grain size $l$ of these films was calculated using the Scherrer formula

$$l = \frac{\lambda}{D\cos\theta}$$

where $D$ is the full width at half maximum of the peak and λ is the wavelength of the X-rays. The typical value of grain size calculated from (1 1 2) peak for these films is 40 nm. Visualisation by SEM [8] has shown that the films exhibit the classical features of the CIGS polycrystalline films and have good adherence to the substrate. This surface morphology was also reported by different authors [9–11]. Guha et al. [11] have observed that the surface roughness of CIGS films determined from the reflectance data and assuming spherical nature of the grains as an approximation [12] decreases with increasing Ga content. In our study, we observed that the films have good compactness and the surface aspect is correlated to the ratio $y = Cu/(In + Ga)$ value. The surface becomes porous with high roughness when $y$ is too much higher than 1. This surface modification is probably due to the formation of some copper based binary compounds.

### 3.2. Electrical properties

The variation of the conductivities with temperature ($\ln\sigma$ versus $10^3/T$) for $CuInSe_2$ and $CuGaSe_2$ is presented in Figs. 3 and 4, respectively.

As it is well known, optical as well as electrical properties, are controlled by the film composition. The determined ratio Cu%/In% for $CuInSe_2$ is 0.79. This composition presents an excess of indium and the most probable intrinsic defect is indium on a copper site. The n-type conductivity of our thin film is then associated with the intrinsic antisite defect $In_{Cu}$ whose formation energy is very low. The main difference between $CuInSe_2$ and $CuGaSe_2$ is the difficulty of obtaining n-type $CuGaSe_2$.

It is observed in Fig. 3 that the conductivity increases slowly in the range 20–150 K while in the high temperature region it is found to increase very sharply. The conductivity value of $CuInSe_2$ at 300 K is 0.17 $cm^{-1}\,\Omega^{-1}$. The values of the activation

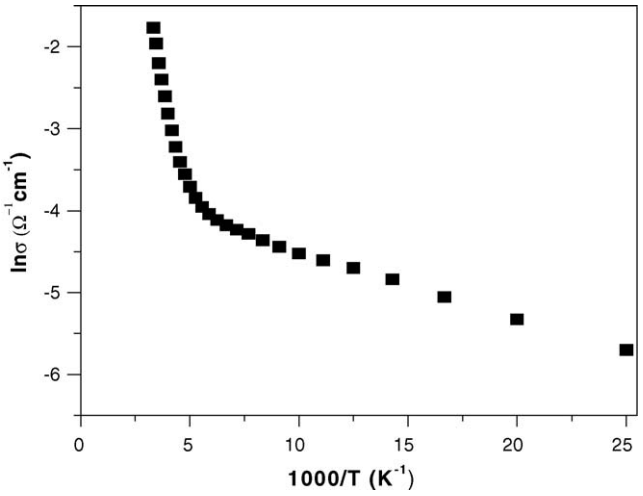


Fig. 3. Experimental variation of conductivity as a function of temperature for $CuInSe_2$.

energies calculated from the Arrhenius plots of the conductivity in the low and high temperature regions are $6.0 \pm 1.8$ and $112 \pm 5$ meV, respectively. The activation energy of the conduction process at low temperatures is low and it can either be due to the conduction from a shallow donor level or due to the predominance of the hopping conduction mechanism. Excitation of shallow levels is unlikely due to the polycrystalline nature of our films. The hopping mechanism arises in grain boundaries when a charge carrier is transferred from a charged trap centre to a neutral one. This process requires thermal activation.

It is difficult to distinguish between thermally activated hopping mechanism having a fixed activation energy ($\sigma = \sigma_0 \exp -\Delta E/kT$) [13,14] and the variable range hopping conduction process. The conduction due to variable range hopping as proposed by Mott [15], is given by

$$\sigma = \frac{\sigma_0}{T^{1/2}} \exp\left[ -\left(\frac{T_0}{T}\right)^{1/4} \right]$$

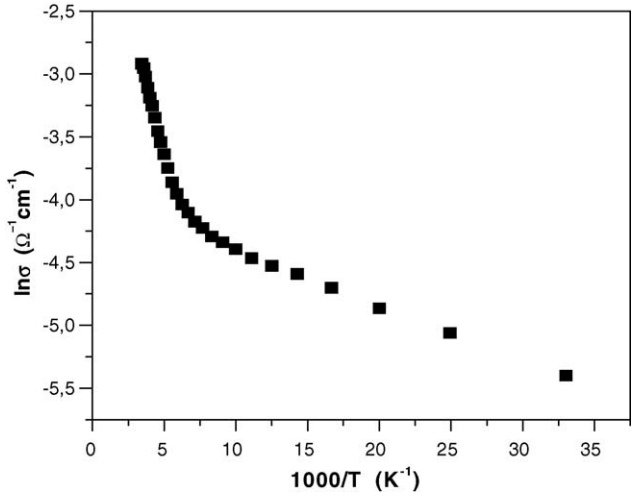


Fig. 4. Experimental variation of conductivity as a function of temperature for $CuGaSe_2$.

The value of $T_0$ is associated with the homogeneity and the disorder in the films. The variable range hopping conduction process requires a value $T_0/T$ higher than 1.

Fig. 5 shows the variation of $\ln \sigma T^{1/2} = f(1/T^{1/4})$. The plot is linear and it is possible that variable range hopping occurs in the grain boundary region of our material. Accordingly, $T_0$ is expressed functionally as [15]

$$T_0 = \frac{\lambda \alpha^3}{kN(E_F)}$$

Here $N(E_F)$, $\lambda$, $\alpha$ and $k$ are, respectively, the density of states at the Fermi level, a dimensionless constant, the decay constant of the wave function of the localized states near Fermi level and Boltzman constant. The experimental calculated value of $T_0 = 1.4 \times 10^5$ is consistent with the proposed model. The pre-exponential factor $\sigma_0$ is given by

$$\sigma_0 = 3e^2 \nu_{ph} \left[ \frac{N(E_F)}{8\pi\alpha k} \right]^{1/2}$$

Here $\nu_{ph}$ is the Debye frequency $\approx 3.3 \times 10^{12}$ [14].

The hopping distance $R$ and energy $W$ are, respectively, given by the following expressions:

$$R = \left[ \frac{9}{8\pi\alpha kTN(E_F)} \right]^{1/4}, \qquad W = \frac{3}{4\pi R^3 N(E_F)}$$

Simultaneous solutions of the above equations when $\lambda = 18$ [13]

$$N_F = 5.55416 \times 10^{10} (\sigma_0)^3 T_0^{1/2} \text{ eV}^{-1} \text{ cm}^{-3}$$

At $T = 100$ K we have

$$\alpha = 64.303 \sigma_0 T_0^{1/2} \text{ cm}^{-1}, \qquad R = \left[ \frac{41.5634}{\alpha N(E_F)} \right]^{1/4}$$

Values of $T_0/T$, $\alpha R \gg 1$ and $W \gg 1$ are presented in Table 1 and compared to previous works [16,17]. The validity of the variable range hopping conduction process is then confirmed since all the conditions are satisfied.

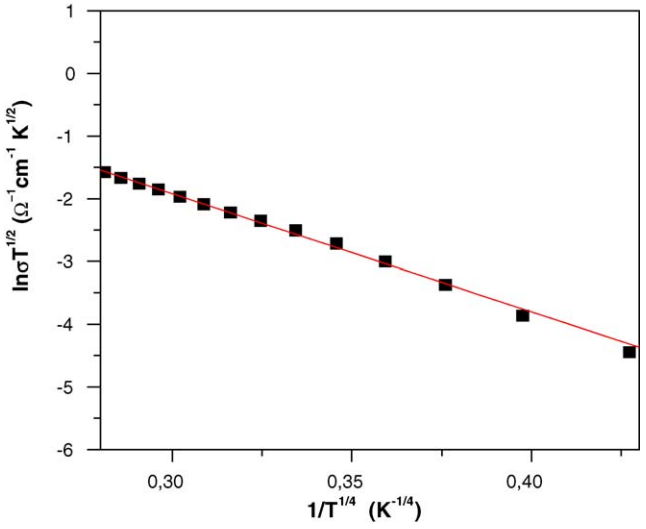


Fig. 5. Variation of $\ln \sigma T^{1/2}$ as a function of $1/T^{1/4}$ for $CuInSe_2$.

Table 1
Mott parameters for the variable range hopping in $CuInSe_2$

| Sample: $CuInSe_2$ | $T_0$ (K) | $N(E_F)$ ($\times 10^{18}$ $eV^{-1}$ $cm^{-3}$) | $R$ at 100 K ($\times 10^{-6}$ cm) | $\alpha$ ($\times 10^{6}$ $cm^{-1}$) | $\alpha R$ | $W$ at 100 K (meV) |
|---|---|---|---|---|---|---|
| [17] | $5.97 \times 10^5$ | 0.62 | 2.72 | 1.21 | 3.3 | 19.13 |
| [16] | | 0.41 | 0.048 (200 K) | | | 19 (200 K) |
| Our result | $1.4 \times 10^5$ | 2.6 | 1.9 | 1.21 | 2.3 | 13.39 |

The high temperature region of the conductivity has been interpreted however in terms of thermoionic emission. In fact, when the temperature is increased the transport results from carriers possessing enough energy to surmount the potential barrier at the grain boundary [18]. The conductivity in this case is given

$$\sigma = \frac{e^2 ln}{(2\pi m^* kT)^{1/2}} \exp\left[-\frac{E_A}{kT}\right]$$

where $n$, $l$ and $m$ are, respectively, the carrier concentration, the average grain size and the density of states effective mass of the carriers. The activation energy $E_A$, which determines the potential barrier height calculated from the variation of $\ln \sigma T^{1/2}$ as a function of $1000/T$ (Fig. 6) is $135 \pm 5$ meV.

For $CuGaSe_2$ thin film, the ratio Cu%/Ga% is 1.09. As expected, it presents a p-type conductivity and a measured conductivity at 300 K of $5.4 \times 10^{-2}$ $\Omega$ $cm^{-1}$. The deduced activation energies from the Arrhenius plots of the conductivity (Fig. 4) in the low and high temperature regions are $4.0 \pm 0.8$ and $40.0 \pm 0.2$ meV, respectively. It is more realistic to interpret these results in connection with the polycrystalline nature of our film. Hence, the transport is governed by the trapping of the carriers in the grain boundaries.

Fig. 7 shows the variation of $\ln \sigma T^{1/2}$ as a function of $1/T^{1/4}$. Table 2 summarises the results of the variable range hopping conduction process for $CuGaSe_2$. The $N(E_F)$ value is somewhat smaller than that found for $CuInSe_2$. This could be interpreted by a probable inaccuracy of the pre-exponential factor $\sigma_0$

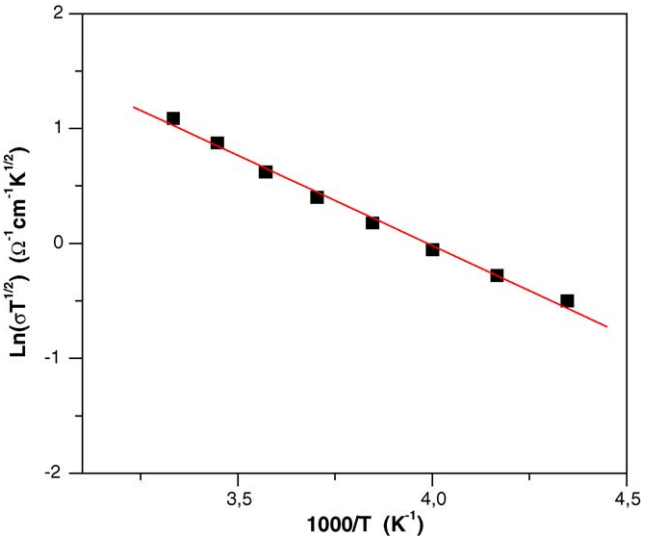


Fig. 6. Variation of $\ln \sigma T^{1/2}$ as a function of $1000/T$.

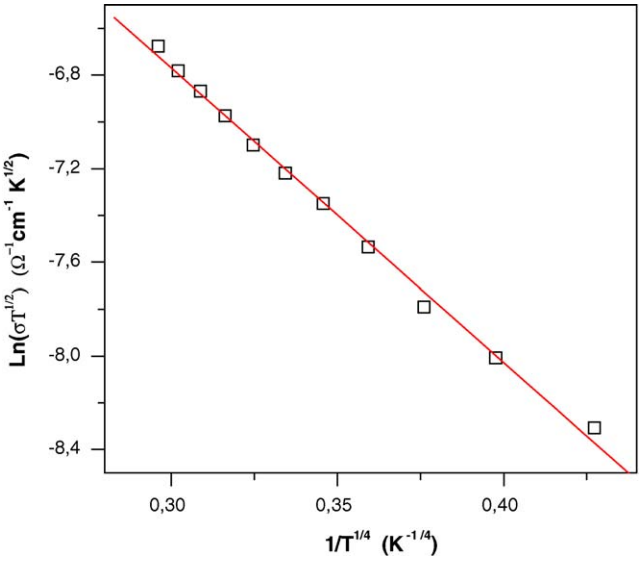


Fig. 7. Variation of $\ln \sigma T^{1/2}$ as a function of $1/T^{1/4}$.

expression. Discrepancies in $N(E_F)$ values for CdTe films were also reported by Lemoine and Mendolia [14].

In the high temperature region, the activation energy deduced from Arrhenius plots presented in Fig. 4 is $40.0 \pm 0.2$ meV. Activation energies of acceptor levels associated with copper and gallium vacancies are, respectively (50–60 meV) [19–21] and (45–56 meV). [22]. However, since our material is polycrystalline in nature, it is unlikely to consider the excitation of the carriers from these defects. So, thermoionic emission is responsible for the increase of the conductivity in this region. Fig. 8 shows the variation of $\ln \sigma T^{1/2}$ as a function of $1000/T$. The deduced activation energy is $50.6 \pm 0.9$ meV. This value compares well with that reported by Gandotra et al. [23].

The special case of conductivity of the mixed compound $CuIn_{1-x}Ga_xSe_2$ ($x$ = Ga/(In + Ga) = 0.13) exhibits a particular behaviour. The Seto model and other classical grain boundary models [24,25] assume that the films are built of identical rectangular grains, in each direction. But, the conductivity of

Table 2
Values of Mott parameters for the variable range hopping in $CuGaSe_2$

| | |
|---|---|
| $T_0$ ($\times 10^4$) | 2.81 |
| $N(E_F)$ ($\times 10^{15}$ $eV^{-1}$ $cm^{-3}$) | 3.99 |
| $R$ at 100 K ($\times 10^{-5}$ cm) | 1.89 |
| $\alpha$ ($\times 10^4$ $cm^{-1}$) | 8.13 |
| $\alpha R$ | 1.54 |
| $W$ at 100 K (meV) | 8.87 |

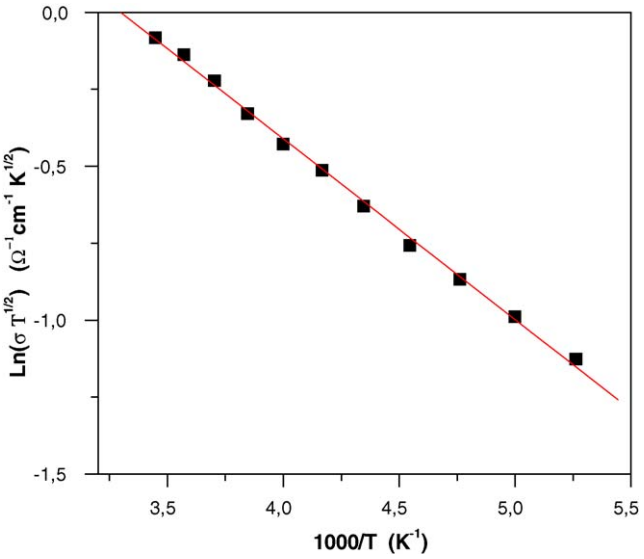


Fig. 8. Variation of $\ln \sigma T^{1/2}$ as a function of $1000/T$.

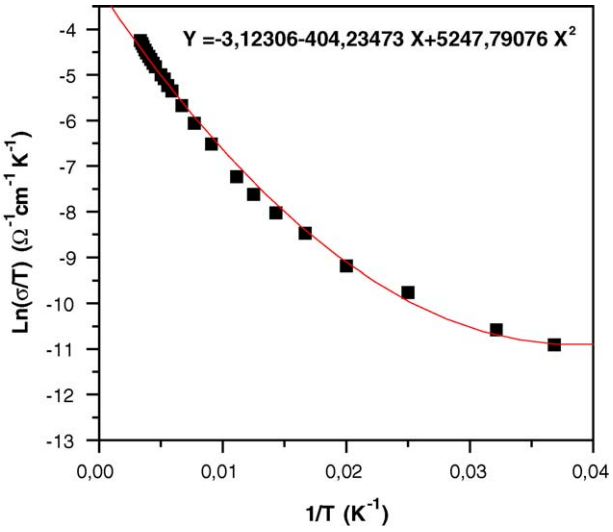


Fig. 9. Curved temperature-dependant conductivity of $CuIn_{1-x}Ga_xSe_2$ thin film.

polycrystalline semiconducting films depends sensitively on the potential barriers and space charge regions that are built up around grain boundaries. This fact has been considered by Werner [26] and interpreted in terms of inhomogeneity of grain boundaries. So the curved Arrhenius plots of the conductivity are due to potential fluctuations of the grain boundaries.

Werner [26] has proposed potential variations among different boundaries and models the fluctuating barriers $\Phi$ by a Gaussian distribution

$$P(\Phi) = \frac{1}{\sigma_\Phi \sqrt{2\pi}} \exp\left[ -\frac{(\bar{\Phi} - \Phi)^2}{2\sigma_\Phi^2} \right]$$

Here $\bar{\Phi}$ denotes the mean barrier and $\sigma_\Phi$ is the standard deviation. The barrier $\Phi$ is replaced by an effective current barrier $\Phi_{\text{eff}}$

$$\Phi_{\text{eff}}(T) = \bar{\Phi}(T) - \frac{\sigma_\Phi^2}{2kT/q}$$

where $k$ is the Boltzman constant and $q$ is the electron charge. The second term of this equation results in a decrease of $\Phi_{\text{eff}}$ upon cooling and consequently the slopes of Arrhenius plots of the conductivity are therefore curved upwards.

Werner [21] has shown that the temperature dependent activation energy is given by

$$E_{\text{A}} = -k \frac{\text{d}}{\text{d}T^{-1}} \ln\left(\frac{\sigma}{T}\right) = q\left(\bar{\Phi}(T=0) - \frac{\sigma_\Phi^2}{kT/q}\right)$$

The temperature dependence of the conductivity is well described by a parabola such as $\ln(\sigma/T) = ax^2 + bx + c$ with $x = 1/T$ (Fig. 9). The values of the standard deviation $\sigma_\Phi$ and the mean potential barrier height $\bar{\Phi}(T=0)$ are obtained from $a$ and $b$. Their respective values are 6.3 and 34.8 mV. We believe that the deduced small value of the potential barrier height is mainly correlated to the high carrier density at 300 K ($n = 1.1 \times 10^{17}\ \text{cm}^{-3}$) of our sample. It is worth noting that Hall measurements were carried out at room temperature by using the Van der Pauw method.

The traps in the grain boundaries are assumed to be initially neutral and become electrically charged after trapping the mobile carriers. Potential barrier at the grain boundary and depletion regions are then created. If the carrier density is smaller than the trapping states, the carriers are almost then trapped. As a result, the measured carrier density must be small and both the resistivity and the potential barrier height values are high. So, we conclude that the high carrier density of our polycrystalline thin film explains well, the derived small value of the potential barrier height. Moreover, the value 6.3 mV of the standard deviation which reflects the potential fluctuation is ascribed to the inherent crystallites distribution of sizes and inhomogeneity of grain boundaries of the studied thin film.

### 3.3. Optical measurements

The absorption coefficient $\alpha$ has been calculated from the measured transmission $T$($\log 1/T = \text{OD}$ (OD: optical density)) of two samples with different thickness:

$$\alpha = \frac{1}{t_2 - t_1} \log\left(\frac{T_1}{T_2}\right)$$

where $t$ is the thickness of the film.

Any errors occurring in the values due the uncertainties induced by this technique are much less than the errors in the thickness measurements that dominate the experimental errors.

$CuInSe_2$ and $CuGaSe_2$ being a direct band gap semiconductors, the plot of $(\alpha h\nu)^2$ versus the photon energy $h\nu$ is reported in Figs. 10 and 11 for the two materials, respectively, since for allowed direct band gap transition, the absorption coefficient $\alpha$ can be related to the photon energy by

$$(\alpha h\nu)^2 = A(h\nu - E_{\text{g}})$$

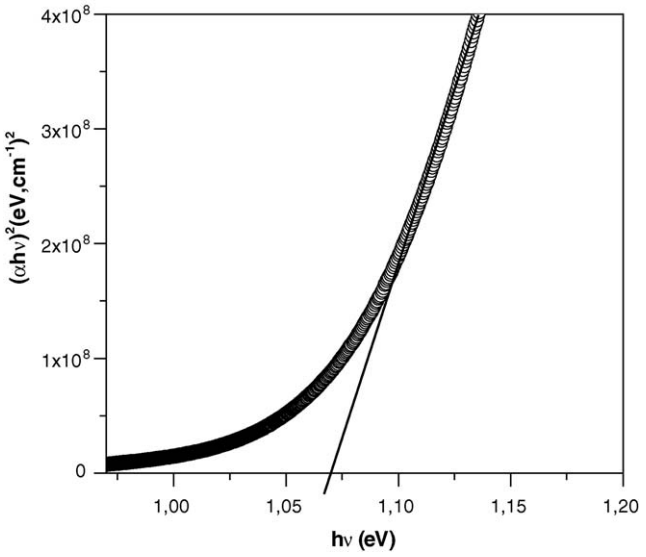


Fig. 10. Plot of $(\alpha h\nu)^2$ vs. $h\nu$ for $CuInSe_2$ thin film.

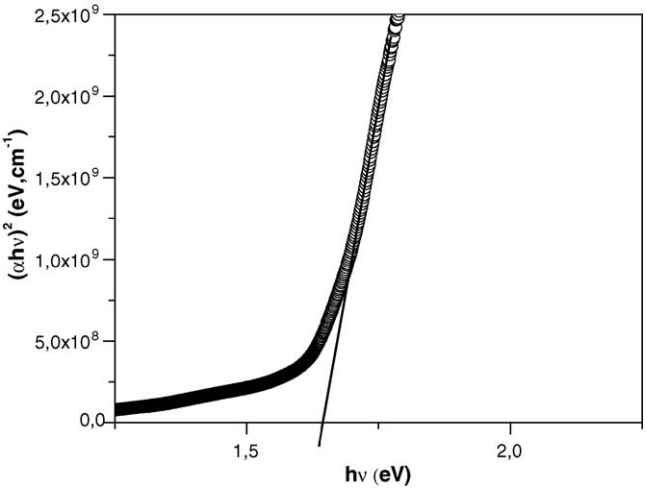


Fig. 11. Plot of $(\alpha h\nu)^2$ vs. $h\nu$ for $CuGaSe_2$ thin film.

where $A$ is a constant which depends on the transition probability and the refractive index, and $E_g$ is the optical energy gap. From the extrapolation of $(\alpha h\nu)^2$ versus $h\nu$ curves to $(\alpha h\nu)^2 = 0$, the average values of the band gap $E_g$ estimated for $CuInSe_2$ and $CuGaSe_2$ are 1.07 and 1.64 eV, respectively. These values compare reasonably well with the results 1.04 and 1.07 eV reported in [27,4], respectively. But the calculated band gap value of 1.07 eV is higher than the value of 1.04 eV usually reported. This is explained by the indium-rich composition of our thin film. It is seen that more indium-rich films have higher energy gaps than less indium-rich ones [28]. If the In/Cu ratio increases, indium occupies some of the copper sites, resulting in antisite defects. The size of the indium atom being larger than that of copper, it would increase the bandgap.

## 4. Conclusion

It is confirmed that the electrical transport of the charge carriers in polycrystalline $Cu(In, Ga)Se_2$ thin films is governed by grain boundaries scattering processes. Hence the conductivity data in the low temperature range for the latter materials is analysed via a variable range hopping. However, thermoionic emission is responsible of the conduction process at high temperature region in both polycrystalline thin films. The conductivity of the particular case of the mixed quaternary thin film is influenced by the fluctuation of the potential barrier induced by the inhomogeneity of the grain boundaries. The direct bandgaps and the high absorption coefficient values of both $CuInSe_2$ and $CuGaSe_2$ confirm that these materials are very suitable for photovoltaic conversion.

## References

[1] U. Rau, H.W. Schock, Appl. Phys. A 69 (1999) 1311.
[2] J. Hedström, H. Ohlsen, M. Bodegard, in: Proceedings of the 23rd IEEE Photovoltaic Specialists' Conference IEEE, New York, (1993), p. 364.
[3] S. Isomura, A. Nagamatsu, K. Shinohara, T. Aono, Solar Cells 161 (1986) 43.
[4] J.L. Shay, B. Tell, H.M. Kasper, L.M. Schiavone, Phys. Rev. B 5 (1972) 5003.
[5] K.W. Mitchell, C. Eberspacher, J.H. Ermer, K.L. Pauls, D.N. Pier, in: Proceedings of the IEEE Photovoltaic Specialists Conference, IEEE, New York, 1985, p. 1733.
[6] J.R. Tutle, D.S. Albin, J. Goral, C. Kennedy, R. Noufi, Solar Cells 2 (1988) 67.
[7] M.A. Contreras, B. Egaas, K. Ramanathan, J. Hiltner, A. Swartzlander, F. Haason, R. Noufi, Prog. Photov. Res. Appl. 7 (1999) 311.
[8] A. Drici, Thèse de Doctorat ès Science, Université d'Annaba, Algérie, 2004.
[9] P. Guha, S.N. Kundu, S. Chaudhuri, A.K. Pal, Mater. Chem. Phys. 74 (2002) 192.
[10] G.W. El Hadj Moussa, Ariswan, A. Khoury, F. Guastavino, C. Llinarés, Solid State Commun. 122 (2002) 195.
[11] S. Roy, P. Guha, S.N. Kundu, H. Hanzawa, S. Chaudhuri, A.K. Pal, Mater. Chem. Phys. 73 (2002) 24.
[12] D. Bhattacharyya, S. Chaudhuri, A.K. Pal, Vacuum 43 (1992) 1201.
[13] N.F. Mott, E.A. Davis, Electronic Processes in Non-crystalline Materials, Clarendon Press, Oxford, 1971.
[14] D. Lemoine, J. Mendolia, Phys. Lett. 82 (1981) 418.
[15] N.F. Mott, Phil. Mag. 19 (1969) 835.
[16] H. Sakata, N. Nakao, Phys. Stat. Sol. (a) 161 (1997) 379.
[17] V.K. Gandotra, K.V. Ferdinand, C. Jagadish, A. Kumar, P.C. Mathur, Phys. Stat. Sol. (a) 98 (1986) 595.
[18] J.Y.W. Seto, J. Appl. Phys. D 46 (1975) 5224.
[19] S.B. Zhang, S.H. Wei, A. Zunger, H. Katayama-Yoshida, Phys. Rev. B 57 (1998) 9642.
[20] J.H. Shön, F.P. Baumgartner, E. Arushanov, H. Riazi-Nejad, Ch. Kloc, E. Bucher, J. Appl. Phys. 79 (1996) 6961.
[21] B.A. Mansour, M.A. El-Hagary, Thin Solid Films 256 (1995) 165.
[22] M. Rusu, P. Gashin, A. Simashkevich, Solar Energy Mater. Solar Cells 70 (2001) 175.
[23] V.K. Gandotra, K.V. Ferdinand, C. Jagadish, A. Kumar, P.C. Mathur, Phys. Stat. Sol. (a) 98 (1986) 595.
[24] G. Baccarni, B. Ricci, G. Spadini, J. Appl. Phys. 49 (1978) 5565.
[25] C.C. Lu, C.Y. Luan, J.D. Meindel, IEEE Trans. Electron Dev. 28 (1981) 818.
[26] J.H. Werner, Solid State Phenom. 37/38 (1994) 213.
[27] M. Gorska, R. Beaulieu, J.J. Loferski, B. Roessler, J. Beal, Solar Energy Mater. 2 (1980) 343.
[28] S.M. Firoz Hasan, M.A. Subhan, Kh.M. Mannan, Opt. Mater. 14 (2000) 329.